Ultrasonics 77 (2017) 54–60

Contents lists available at ScienceDirect

Ultrasonics

journal homepage: www.elsevier.com/locate/ultras

Acoustic power delivery to pipeline monitoring wireless sensors

M.E. Kiziroglou *, D.E. Boyle, S.W. Wright, E.M. Yeatman

Department of Electrical and Electronic Engineering, Imperial College London, London SW7 2AZ, United Kingdom

ARTICLE INFO

Article history:
Received 10 May 2016
Received in revised form 18 January 2017
Accepted 19 January 2017
Available online 23 January 2017

Keywords:
Wireless power transfer
Ultrasonic
Acoustic
Pipeline
Monitoring
Sensor

ABSTRACT

The use of energy harvesting for powering wireless sensors is made more challenging in most applications by the requirement for customization to each specific application environment because of specificities of the available energy form, such as precise location, direction and motion frequency, as well as the temporal variation and unpredictability of the energy source. Wireless power transfer from dedicated sources can overcome these difficulties, and in this work, the use of targeted ultrasonic power transfer as a possible method for remote powering of sensor nodes is investigated. A powering system for pipeline monitoring sensors is described and studied experimentally, with a pair of identical, non-inertial piezoelectric transducers used at the transmitter and receiver. Power transmission of 18 mW (Root-Mean-Square) through 1 m of a 118 mm diameter cast iron pipe, with 8 mm wall thickness is demonstrated. By analysis of the delay between transmission and reception, including reflections from the pipeline edges, a transmission speed of 1000 m/s is observed, corresponding to the phase velocity of the L(0,1) axial and F(1,1) radial modes of the pipe structure. A reduction of power delivery with water-filling is observed, yet over 4 mW of delivered power through a fully-filled pipe is demonstrated. The transmitted power and voltage levels exceed the requirements for efficient power management, including rectification at cold-starting conditions, and for the operation of low-power sensor nodes. The proposed powering technique may allow the implementation of energy autonomous wireless sensor systems for monitoring industrial and network pipeline infrastructure.

1. Introduction

Remote powering of wireless sensors can resolve the main limiting factor in the widespread adoption of wireless sensor network (WSN) technologies. The maintenance and environmental burden of battery usage has become more important, despite the significant energy density increases of the last decade, because of the expansion of applications requiring the permanent installation of a large number of sensors. Examples include industrial monitoring for optimized maintenance and control, smart management of urban infrastructure, and monitoring of resource distribution networks for reliability and security.

Energy harvesting, the exploitation of environmental energy that is locally available to a sensor, has been demonstrated to considerably enhance energy autonomy of a diverse range of wireless systems. The available energy is adequate in a number of cases, but typically requires the development of bespoke harvesting devices. This requirement inhibits the adoption of energy harvesting solutions in commercial systems.

The case of motion energy harvesting is a representative example. Enough energy is available in a wide range of environments, including industrial, vehicle and infrastructure equipment. In addition, the micro-electro-mechanical systems (MEMS) technology required for the production of motion micro generators is sufficiently advanced. However, each application has a different vibration spectrum, and different power and size specifications, requiring a customized implementation. In order to solve this problem, a number of promising techniques have been proposed, such as frequency up-conversion based on bi-stable systems [1], non-linear (broadband) mechanical oscillators [2], pre-biasing of piezoelectric transducers [3], pre-loading of cantilevers with mechanical compression [4], and free-mass non-resonant devices [5]. Effectively, these approaches reduce the maximum possible energy density in exchange for broadband operation and hence broader applicability.

In a different approach proposed here, the high-performance of vibration energy harvesters at resonance can be exploited by inducing vibration at a suitably selected frequency into the sensor environment. Thereby, a resonant powering system suitable for a range of environments such as those involving flat or longitudinal solid structures can be developed. This approach is similar in con-

* Corresponding author.
E-mail address: m.kiziroglou@imperial.ac.uk (M.E. Kiziroglou).

http://dx.doi.org/10.1016/j.ultras.2017.01.017
0041-624X/

cept to the tuning of RF harvesting devices to the central WiFi/GSM frequencies or to a dedicated RF power transmitter [6,7].

Acoustic power transfer has been under investigation in recent years for power delivery through metal enclosures, biological tissues, and through air. Various through-wall systems delivering more than 50 W at greater than 50% efficiency have been demonstrated, while also incorporating communication capabilities [8,9]. As an example, Leung et al. have recently demonstrated 74% efficient acoustic power delivery of 62 W, through a 70 mm thick aluminium panel, using 28 kHz Langevin transducers [10]. Ozeri et al. demonstrated through-tissue power delivery of 100 mW with 39% efficiency at 5 mm distance, and 45 mW at 40 mm [11]. A comparison between acoustic and inductive power transfer for biomedical implants has shown that the former will be more efficient for longer distances and small receivers [12]. Finally, contactless acoustic power transfer at short distances has recently been studied by Shahab et al. at Georgia Tech [13]. A review of acoustic energy transfer works including an analytical model of through-wall systems can be found in [8].

Acoustic power transfer through solid structures may also be applicable for longer distances, depending on the geometry and the type of material. While highly efficient transfer may be impractical to accomplish, especially when using application-defined, unmodified structures, the aforementioned vibration transmitter and receiver approach may allow the use of one or more tuned harvesting devices, which have been shown to provide sufficient energy density for the operation of wireless sensor networks [14,15].

In a previous paper, a proof of concept of acoustic power transfer through cast iron water pipes was presented, and the acoustic impedance matching was analyzed with respect to efficient and non-intrusive mounting of devices [16]. A power delivery of 330 μW at 1 m distance was demonstrated, using a 48.5 kHz signal. The intended application is the powering of multiple buried sensors (e.g. corrosion sensors) from an accessible section of pipe. Here, a further developed implementation is used, with an improved device mounting method, to analyze the acoustic transmission in more detail. The effect of filling the pipeline with water is also experimentally studied, and discussed in relation to the transmission spectrum and power level. The profile of the received signal is analyzed with respect to transmission speed of the main acoustic modes for pipeline structures, and reflection at mounting points. The scaling of received power with the transmitted signal intensity is studied experimentally and conclusions are drawn regarding the applicability of this technique to powering pipeline monitoring sensor systems for different classes of infrastructure.

2. System concept

The proposed concept of acoustic-powered pipeline sensors is schematically described in Fig. 1. A power transmitter device is attached externally to the pipe surface. Through an impedance matching acoustic contact, it can inject vibrations into the pipeline structure at a chosen frequency.

Depending on the mounting method, the vibration is transmitted along the pipeline, through the pipeline wall or through the fundamental guided acoustic modes of the cylindrical structure, i.e. the axial (longitudinal) L(0,1), radial (transverse) F(1,1), or torsional T(0,1) modes. In the case of a liquid-filled pipeline, transmission is also possible through the liquid. These modes and their dispersion characteristics have been extensively studied [17]. It has been shown that the dispersion curves depend on the radius of the cylindrical structure. In the case of an embedded pipeline, attenuation of the L(0,1) and F(1,1) modes occurs mainly by leakage to the surrounding material. The water borne mode however

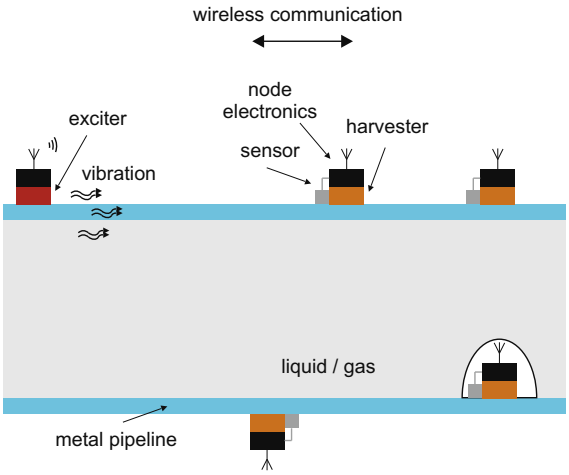

Fig. 1. Conceptual description of powering pipeline sensors through acoustic waves.

experiences lower attenuation, offering longer propagation distances. A complete study of pipeline acoustic modes, including attenuation in soil-embedded structure can be found in [17].

One or more acoustic harvesters installed at a distance along the pipeline and tuned to the transmitter frequency can receive a portion of the acoustic power that is available in the pipeline, either for direct use or for storage and subsequent use within a desired sensing and data transmission scheduling scheme.

The power transmitter may be integrated into the local communications server, which controls and concentrates the measured data. The efficiency of RF wireless communication between the data concentrator and the sensors will depend on the surrounding environment. In cases where RF transmission is obscured, such as in buried pipelines, the acoustic power transmission may be modulated to carry control or other information signals.

3. Experimental setup

In order to study the proposed power delivery method and evaluate its performance on common pipeline structures, an evaluation setup was developed, using a 1.8 m long, 118 mm diameter cast iron tube, with a wall thickness of 8 mm. This type of pipeline is commonly used in existing urban water distribution infrastructures, such as Thames Water's distribution network in London, U. K. The pipe was supported by two 150 × 150 × 50 mm polystyrene

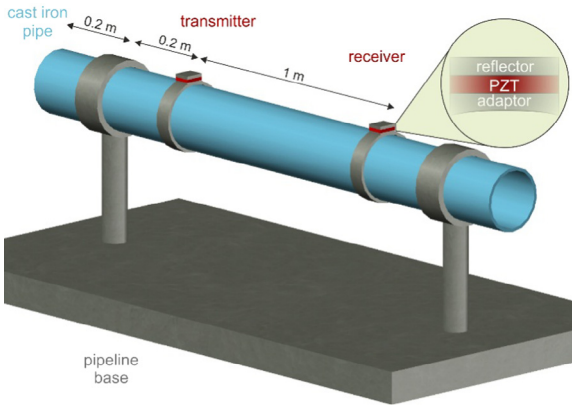

Fig. 2. Experimental setup concept used for evaluation of acoustic power transfer through cast iron pipe.

pads centered at a distance of 200 mm from the pipe ends. A schematic description of this experimental setup is presented in Fig. 2.

A practical exciter/receiver installation method usually requires more than one points of contact. In designing transducers customized for particular transmission modes, these points of contact must be selected with precision, taking into account the propagation speed and phase of the acoustic wave. In turn, this would imply specific frequency bands, which is fine for an optimized product design but not convenient for a broadband power transfer study. Therefore, for the implementation developed and used in the present work, a simple PZT layer and acoustic matching design is employed, with an aluminium reflector and adaptor as depicted in Fig. 2. This design allows the transfer of both the axial and radial modes of the PZT disk to the radial, F(1,1), and longitudinal, L(0,1), modes of the pipe structures respectively. The PZT disk was selected to suit the size of typical embedded sensors and the pipe diameter, but also to achieve a large vibration displacement and thereby reduce the effect of interface gaps.

The power transmitter consists of an APC International Ltd PZT 850 disk with diameter 48 mm and thickness 7.9 mm, stacked between a 60 × 60 × 20 mm aluminium reflector on top, and an aluminium adaptor of the same size with a concave underside. The density, dielectric constant and voltage constant of the PZT 850 material are 7600 kg/m^3, 1900 and 26.8 mV/m respectively [14]. The disk dimensions correspond to radial and axial resonance at 50 kHz and 300 kHz respectively [16]. The electrical impedance of the PZT disk was measured before installation. The results are plotted in Fig. 3, demonstrating the expected radial and axial resonance and corresponding harmonics. The effect of installation to the impedance spectrum is to smoothen the resonance peaks, due to the resulting mechanical coupling between the disk and the structure [16].

An image illustrating the transmitter, pipe and receiver is shown in Fig. 4. Therein, a red hook-and-loop strip is used for clamping. For the experimental evaluation presented in this paper, a G-clamp was used with silicone grease at the interface to improve acoustic coupling. The transmitter was mounted at a distance of 400 mm from one end. An identical stack was used at the receiver, mounted in the same way, 400 mm from the other end of the pipe. The distance between the centers of the transmitter and the receiver was 1 m.

A block diagram of the transmitter driver and measurement systems used during the experiments is shown in Fig. 5. A signal generator and a Falco WMA-300 high voltage amplifier were used to drive the PZT ceramic, through a 4 W, 27 Ω resistor to allow monitoring of the current. The voltage and current of the transmitting transducer were monitored using an oscilloscope. The voltage at the detector was also monitored by an oscilloscope, in both open circuit and loaded conditions. A 0–10 kΩ variable resistor was used as the load, allowing the determination of the optimal load value for maximum real power delivery.

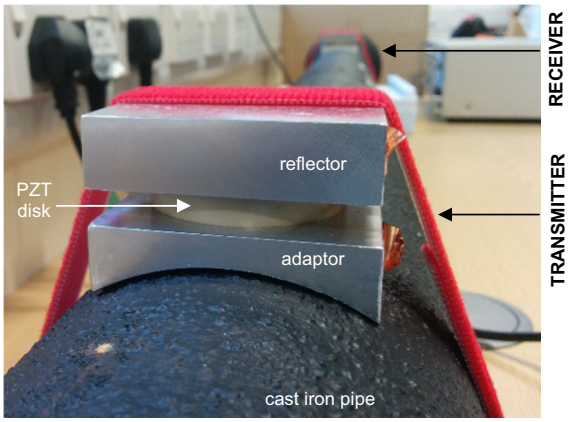

Fig. 4. Image of the experimental setup showing the transmitter transducer stack. The receiver is also visible, at the other end of the test pipe.

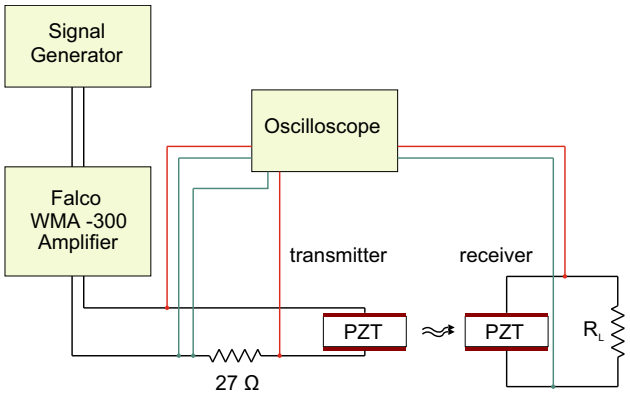

Fig.5. Block diagram of the driving and measuring circuit.

4. Power transmission

A series of experiments was performed to study various aspects of the proposed method. This study included the maximum power delivery that can be demonstrated by this setup, the delay and timing of different wave components arriving at the receivers, the effect of water filling and the scaling of output power with input power.

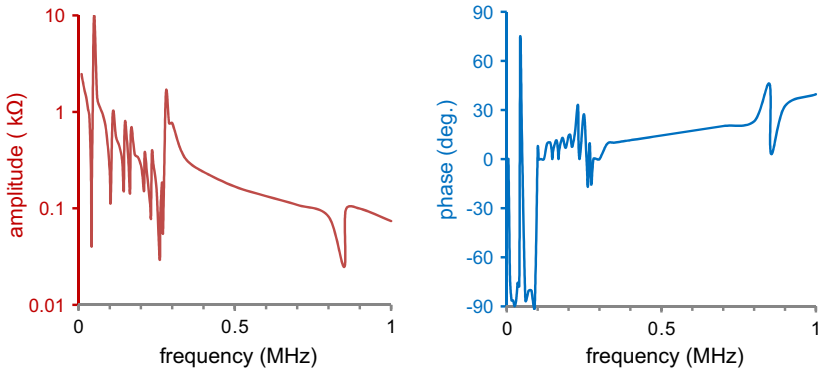

Fig.3. Measured impedance amplitude (left) and phase (right) of the PZT disk.

In all experiments the maximum power delivery was observed for a drive frequency of approximately 48 kHz. This corresponds to the resonance of the Mason model of the Ø 48 mm PZT disk, in the radial direction [16]. A plot of the voltage input at the transmitter and the voltage output at the receiver measured across a 1 kΩ resistive load, is shown in Fig. 6. The input and output amplitudes are 150 V and 6 V respectively. This corresponds to continuous Root-Mean- Square (RMS) power of 18 mW delivered to the receiver load. This compares well with the power requirements of sensor nodes, which depending on the sensing scenario and the type of sensor can have an average power demand in the range between 0.1 mW and 100 mW. Moreover, the voltage output is high enough to support efficient direct passive rectification. This is critical because it allows cold-starting, which is a highly desirable feature of energy autonomous systems.

5. Wave modes and delay analysis

Given the short length of the pipe sample used in the laboratory, reflections from the ends may play an important role in the power that is picked up by the receiver. This can be examined by modulating the excitation at the transmitter with a pulsed signal and analysis of the waveform shape at the receiver. A 2 ms pulse excitation at 47.5 kHz is shown in Fig. 7. The shape of the received signal indicates the existence of more than one received pulse. The delay between the transmission start and the start of the received pulse is 1 ms. Given that the distance between the transmitter and the receiver is 1 m, this delay indicates a wave speed of 1000 m/s, which corresponds to the speed of the first order axial, L(0,1) and radial, F(1,1), modes of iron pipes for this frequency range, as predicted by Long et al. [17].

The bulk cast iron propagation speed of longitudinal waves is 4600 m/s. Such a fast signal is not observed in the results of Fig. 7. At this speed and the operating frequency of 47.5 kHz, the bulk wavelength would be ≈10 cm; since this is more than 10× the wall thickness, such bulk waves would not be expected to propagate. In order to analyze the morphology of the received signal, propagation through the fluid inside the pipeline should be considered, as well as the expected reflections coming from the pipeline ends and mounting points. To assist this analysis, the velocities of different modes of vibration transmitted through the cast iron pipe and the filling fluid are summarized in Table 1.

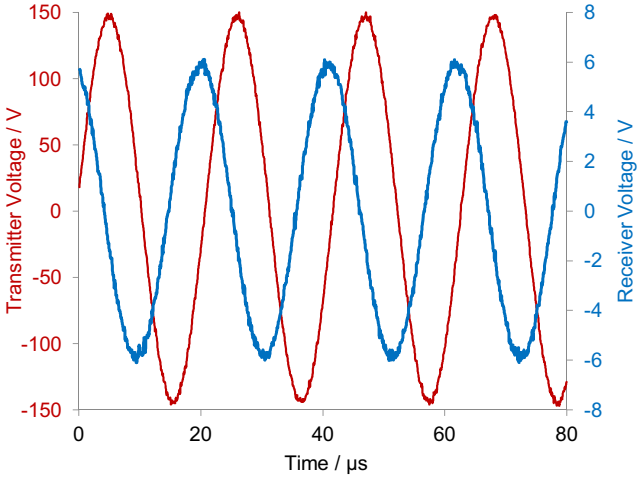

Fig. 6. Transmitter and receiver voltage at 47.5 kHz, at a distance of 1 m. A continuous received signal with amplitude 6 V on a 1 kΩ load demonstrates 18 mW (RMS) of received power.

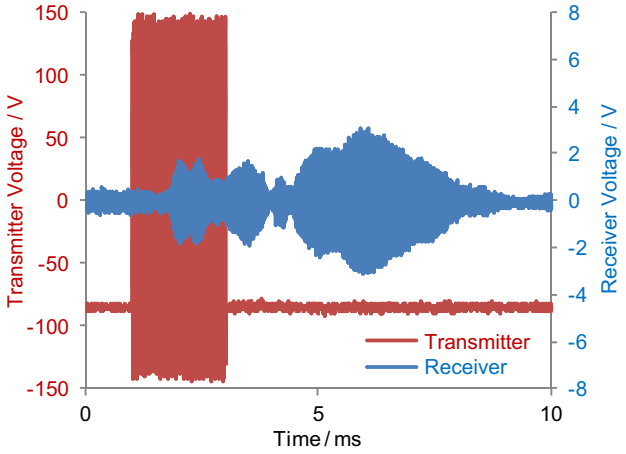

Fig. 7. Transmitter and receiver voltages at 47.5 kHz, with an 1 kΩ receiver resistor, for a separation of 1 m, using pulse modulation to study the morphology of the received signal.

Table 1
Speeds of vibration propagation through cast iron pipelines.

Mode	Value (m/s)
Bulk cast iron longitudinal wave	4600
Axial (longitudinal) wave L(0,1)[a]	1000
Radial (transverse) wave F(1,1)[a]	1000
Air at 20 °C	343
Water at 20 °C	1482

[a] For a frequency-radius product >1 MHz mm [17].

An analysis of the expected time of arrival of the main signals contributing to the received waveform are plotted in Fig. 8. In this analysis, only the timing is studied; signal attenuation and reflection efficiency are not considered, and hence a discretized amplitude is used to indicate signal presence or absence. The signal generated at the transmitter creates waves traveling in both right and left directions. After 1 ms, the right-traveling wave arrives at

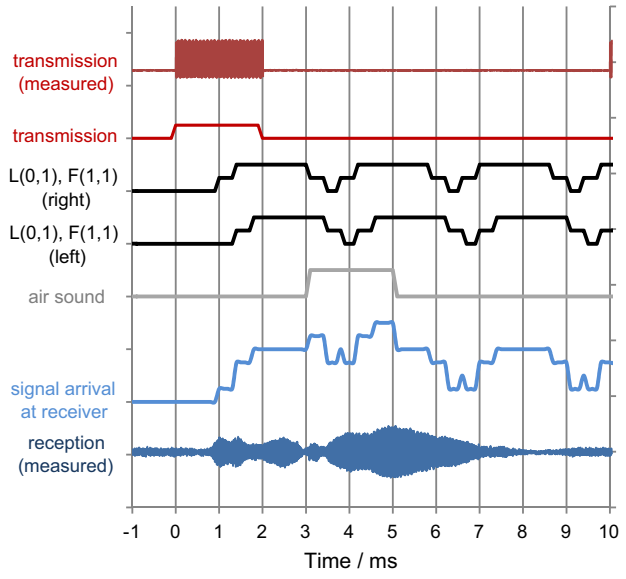

Fig. 8. Analysis of the experimental data of Fig. 7 by comparison with the expected arrival times of different transmission modes, including expected reflections from the pipe mounting points.

the receiver. The left wave is expected at the receiver 0.4 ms later, as it travels a distance of 0.2 m leftward, gets reflected by the left mounting point, and then travels rightward for 1.20 m (see Fig. 2 for a geometry reference). The reflection of the right wave from the right mounting point also arrives at t = 1.4 ms. In addition, the portion of the signal traveling through air arrives at t = 3 ms and, as the tube is open from both sides, does not include significant reflections. A curve showing the overlapping of different signals is shown in Fig. 8 (light blue in the electronic edition), with label "Signal arrival at receiver", in comparison with the measured signal. According to this analysis, the first 2 ms part of the received signal (from t = 1 ms to t = 3 ms) can be attributed to the L(0,1) and F(1,1) modes of the pipe, and to their reflections. This is repeated again at the receiver, starting at t = 3.8 ms, after the signals have completed a full cycle along the pipe. From t = 3 to 5 ms, the air contribution is also expected to be present, increasing the number of overlapping signals. More echoes of pipeline modes follow, at t = 6.6 ms, t = 9.4 ms, etc., without the air signal's contribution. It is noted that the air contribution to the signal at the receiver is expected to be very small, due to the large impedance mismatch at the metal-air interfaces. On the other hand, the effect of the fluid contained by the pipeline to the acoustic power propagation can be significant, especially in the case of water or other liquids. The effect of water filling is studied experimentally in the following section.

6. The effect of water filling

The effect of filling the pipeline with a liquid on power transmission was studied by measuring the receiver voltage for different transmission frequencies, for the cases of empty, quarter-full, half-full and full pipeline, using water. The resulting spectra for the different cases are shown in Fig. 9. A uniform reduction in voltage amplitude across the spectrum is observed for increasing water levels. It is concluded that the liquid filling increases the attenuation of the transmitted vibration throughout the spectrum. Nevertheless, the power delivery and the voltage amplitude at the receiver remain in the desired range, i.e. >1 mW and 1 V, respectively, in all cases.

The delay analysis method introduced in Section V for the case of transmission through an empty pipe is also applied here to evaluate the role of different vibration transmission modes. This analysis is shown in Fig. 10. The expected arriving times for the cast iron pipeline modes and their reflections are the same as in Fig. 8. However, the fluid contribution now propagates at a much higher speed (1482 m/s) and experiences reflection at the pipeline edges. Its right-traveling portion is expected to arrive at the receiver for the first time at 0.7 ms, a bit faster than L(0,1) and F(1,1). It overlaps with the arrival of the left-traveling fluid wave, which arrives at t = 1.2 ms, and with the first incidence of the cast iron wave packets and their reflection from the right mounting point. This overlap gives the largest expected waveform between t = 1 ms and t = 3 ms, which is in line with the experimentally measured peak also shown in Fig. 9. The second incidence of the waves is expected to occur between t = 3.2 and 5.2 ms. This again agrees with the experimentally observed signal, which is significantly attenuated. After that, the timing is more irregular, as the velocity and traveling length differences lead to a phase shift between the water and iron wave packets.

Overall, this analysis provides an explanation of the doubling of the measured signal duration at the receiver (2 ms compared to the 1 ms of the transmission signal, in both occurrences). It also shows that in contrast to the air-filled pipeline experiment, in the case of water, the first arriving wave packet is expected to have the highest amplitude, as is experimentally observed.

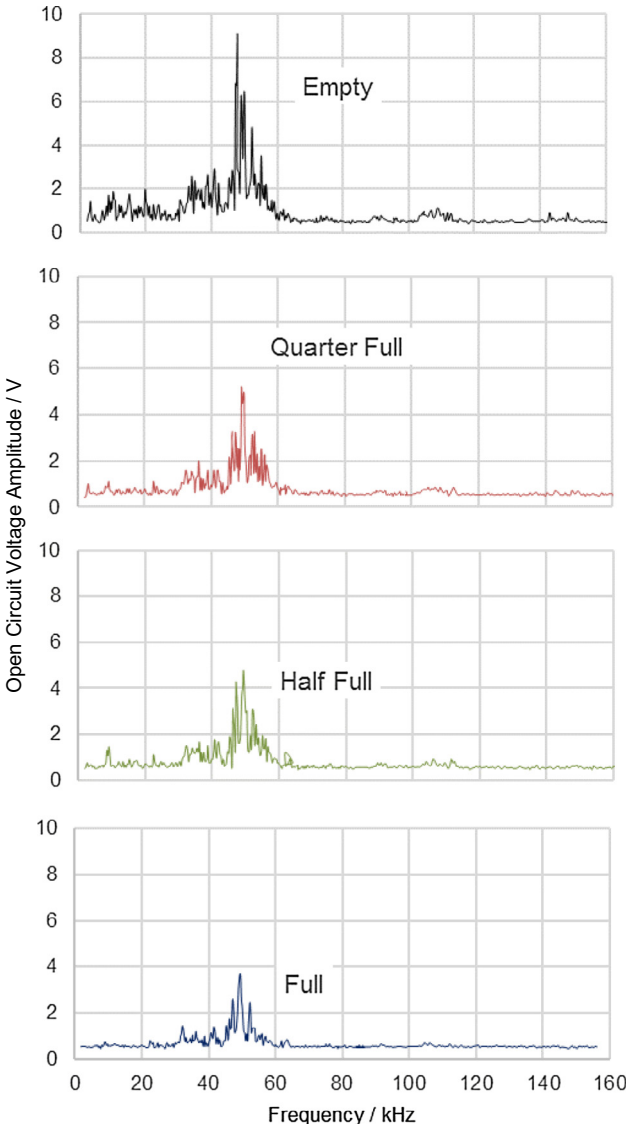

Fig. 9. Received voltage as a function of frequency for different pipe water levels. The spectral profile is similar but an attenuation increase with water level is observed.

7. Voltage and power scaling

The power requirements of sensor nodes vary with the application scenario. In some cases continuous power delivery may be required, while in others the periodic charging of a sensor node may be preferable. In the design of a particular power delivery system based on acoustic power transfer through structures, the following points should be considered:

- The transmitter can be permanently installed or portable (e.g. a portable charger).
- The voltage and power level at the transmitter must be optimized according to the sensor energy and to the transmitter portability requirements.
- Depending on the sensor node operation cycle and the sensor type, the average required acoustic power can be significantly lower than 1 mW.
- For lower power applications, the voltage at the receiver needs to be adequate for passive rectification, at least at the beginning of charging, for cold starting.

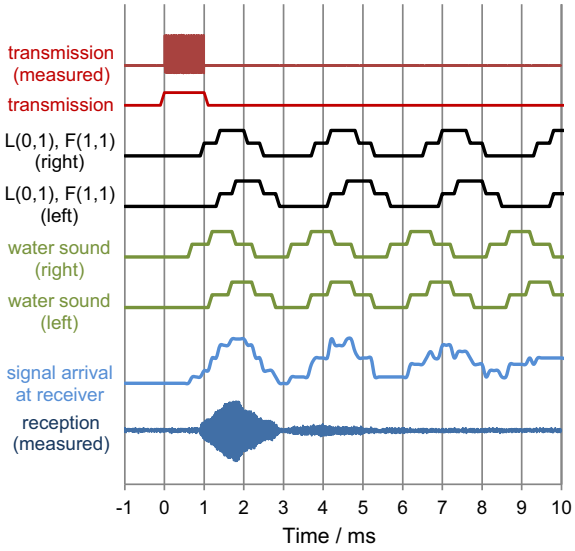

Fig. 10. Analysis of pulse modulated excitation data at 47.5 kHz, from the fully water-filled pipeline, by comparison with the expected arrival times of different transmission modes, including expected reflections from the pipe mounting points and edges.

In order to investigate power scaling of the proposed method, the receiver voltage was measured at open-circuit and in connection to a resistive load, for different voltages applied at the transmitter. The measurements were performed using a continuous sinusoidal 47.5 kHz signal. The voltage and current at the transmitter were monitored by an oscilloscope and the power input was calculated from the amplitudes of the measured voltage and current waveforms, and their phase difference θ:

$$P_{IN} = I_{IN,RMS} \cdot V_{IN,RMS} \cdot \cos\theta \quad (1)$$

The receiver output power was calculated from the voltage amplitude measured on a $R_L = 750\,\Omega$ resistive load, selected for maximum power transfer by matching the measured output impedance of the receiver PZT:

$$P_{OUT} = \frac{V_{OUT,RMS}^2}{R_L} \quad (2)$$

More specifically, the resistive load was selected by measuring the voltage on a variable resistor connected to the receiver. The maximum power transfer point corresponds to a load resistance equal to the output impedance amplitude of the PZT element. It can be determined by setting the voltage observed on the load at half the open-circuit voltage value. The power delivery efficiency could be further improved by using active load power management techniques such as pre-biasing [3].

The voltage measured at the receiver load is plotted as a function of transmitter voltage in Fig. 11. The results demonstrate a near linear scaling, with the maximum voltage observed for this set of measurements being 5.25 V, for 150 V at the transmitter. For a transmission of amplitude 5 V, the measured voltage amplitude on the load was 115 mV. The corresponding plot of received power as a function of transmitter real power is shown in Fig. 12. A near-linear scaling is again observed, corresponding to a power delivery efficiency of 0.1%. This low efficiency could be improved, for example by improving the transducer-to-pipe coupling, or by using larger, more efficient or multiple receiver devices. The latter case would be convenient for the installation of a number of sensor nodes, powered by a common transmitter.

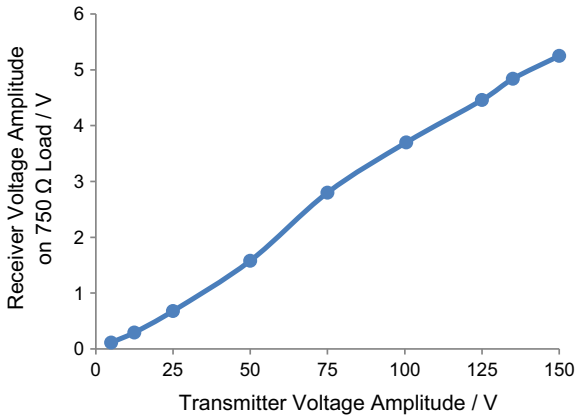

Fig. 11. Measured voltage amplitude on a 750 Ω resistive load as a function of voltage amplitude applied at the transmitter, at a distance of 1 m, using a 47.5 kHz signal.

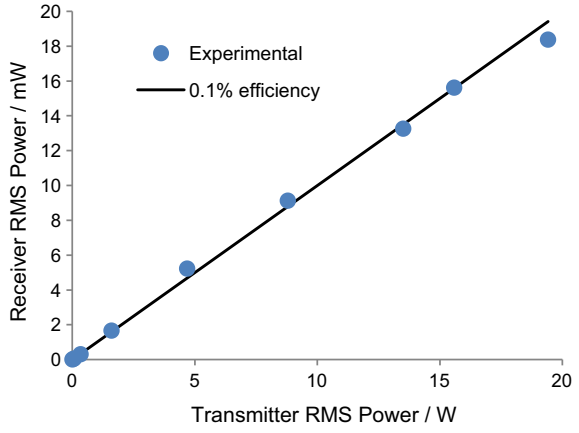

Fig. 12. Received vs transmitted RMS power at a distance of 1 m, using a 47.5 kHz signal, corresponding to the voltage measurements of Fig. 11.

8. Conclusion

The experimental results presented in this paper show that acoustic waves of substantial power can be injected into metallic pipelines, by simple non-inertial piezoelectric exciter structures. The waves travel along the pipeline at a speed of around 1000 m/s, corresponding to the first longitudinal and radial pipe acoustic modes. Continuous power delivery of 18 mW (RMS) is demonstrated, over a distance of 1 m, using a 47.5 kHz signal and a piezoelectric receiver identical to the transmitter. The effect of water-filling on the power transfer spectrum was studied showing a reduction of received power. At full-filling, power delivery over 4 mW is still demonstrated. Acoustic reflections from mounting points and the ends of the pipe overlap with the direct wave, allowing an increase of power delivery during continuous transmission. In longer installations, reflections may play a significant role only in the vicinity of reflection points. The received power and voltage levels are adequate for efficient power management, including rectification and storage, and for powering typical low power sensor node systems. Specific power management techniques such as the use of a reactive load at the receiver could further improve the efficiency of power reception.

Low bit-rate data communication can potentially be achieved through the acoustic power delivery signals, building on previously reported acoustic communication techniques [18]. In this direction, a study of the dispersion characteristics of the main propaga-

tion modes for different pipeline filling conditions would be desirable. Such a study could be performed by applying the Disperse software that is available by the non-destructive evaluation group of Imperial College London [19], and would also be helpful towards more specific exciter and receiver device designs.

The acoustic power delivery method proposed in this work may allow the implementation of energy-autonomous, low-duty-cycle pipeline monitoring systems for industrial distribution infrastructure [20,21].

Acknowledgements

This work has been partially supported by the European Union EIT Digital (15171) and RCUK/EPSRC (EP/I038837/1).

References

[1] R.L. Harne, K.W. Wang, A review of the recent research on vibration energy harvesting via bistable systems, Smart Mater. Struct. 22 (2013) 023001.
[2] D.A.W. Barton, S.G. Burrow, L.R. Clare, Energy harvesting from vibrations with a nonlinear oscillator, J. Vib. Acoust. 132 (2010), 021009-021009.
[3] J. Dicken, P.D. Mitcheson, I. Stoianov, E.M. Yeatman, Power-extraction circuits for piezoelectric energy harvesters in miniature and low-power applications, IEEE Trans. Power Electron. 27 (2012) 4514–4529.
[4] S.L. Eli, K.W. Paul, Resonance tuning of piezoelectric vibration energy scavenging generators using compressive axial preload, Smart Mater. Struct. 15 (2006) 1413.
[5] M.E. Kiziroglou, C. He, E.M. Yeatman, Rolling rod electrostatic microgenerator, IEEE Trans. Industr. Electron. 56 (2009) 1101–1108.
[6] R. Vullers, H. Visser, B.O het Veld, V. Pop, RF harvesting using antenna structures on foil, in: Proc. PowerMEMS 2008+ microEMS, 2008, pp. 9–12.
[7] X. Lu, P. Wang, D. Niyato, D.I. Kim, Z. Han, Wireless networks with rf energy harvesting: a contemporary survey, IEEE Commun. Surv. Tutorials 17 (2015) 757–789.
[8] M.G.L. Roes, J.L. Duarte, M.A.M. Hendrix, E.A. Lomonova, Acoustic energy transfer: a review, IEEE Trans. Industr. Electron. 60 (2013) 242–248.
[9] M. Kluge, T. Becker, J. Schalk, T. Otterpohl, Remote acoustic powering and data transmission for sensors inside of conductive envelopes, in: Sensors, IEEE, 2008, pp. 41–44.
[10] H.F Leung, B.J Willis, A.P Hu, Wireless electric power transfer based on Acoustic Energy through conductive media, in: 2014 IEEE 9th Conference on Industrial Electronics and Applications (ICIEA), 2014, pp. 1555–1560.
[11] S. Ozeri, D. Shmilovitz, S. Singer, C.-C. Wang, Ultrasonic transcutaneous energy transfer using a continuous wave 650 kHz Gaussian shaded transmitter, Ultrasonics 50 (2010) 666–674, 6.
[12] A. Denisov, E. Yeatman, Ultrasonic vs. inductive power delivery for miniature biomedical implants, in: 2010 International Conference on Body Sensor Networks (BSN), 2010, pp. 84–89.
[13] S. Shahab, M. Gray, A. Erturk, Ultrasonic power transfer from a spherical acoustic wave source to a free-free piezoelectric receiver: modeling and experiment, J. Appl. Phys. 117 (2015) 104903.
[14] S.P. Beeby, M.J. Tudor, N. White, Energy harvesting vibration sources for microsystems applications, Meas. Sci. Technol. 17 (2006) R175.
[15] P.D. Mitcheson, T.C. Green, E.M. Yeatman, A.S. Holmes, Architectures for vibration-driven micropower generators, J. Microelectromech. Syst. 13 (2004) 429–440.
[16] M.E. Kiziroglou, D.E. Boyle, S.W. Wright, E.M. Yeatman, Acoustic energy transmission in cast iron pipelines, in: PowerMEMS 2015, Journal of Physics: Conference Series 660, 012095, 2015. http://dx.doi.org/10.1088/1742-6596/660/1/012095.
[17] R. Long, M. Lowe, P. Cawley, Attenuation characteristics of the fundamental modes that propagate in buried iron water pipes, Ultrasonics 41 (2003) 509–519, 9.
[18] G. Kokossalakis, Acoustic Data Communication System for In-pipe Wireless Sensor Networks Ph.D., Department of Civil and Environmental Engineering, Massachusetts Institute of Technology, Boston, MA, USA, 2006.
[19] B. Pavlakovic, M. Lowe, D. Alleyne, P. Cawley, Disperse: a general purpose program for creating dispersion curves, Rev. Prog. Quant. Nondestruct. Eval. 16 (1997) 185–192, http://dx.doi.org/10.1007/978-1-4615-5947-4_24.
[20] M.I Mohamed, W.Y Wu, M. Moniri, Power harvesting for smart sensor networks in monitoring water distribution system, in: 2011 IEEE International Conference on Networking, Sensing and Control (ICNSC), Dover, 2011, pp. 393–398.
[21] A. Nasir, B.H Soong, PipeSense: a framework architecture for in-pipe water monitoring system, in: 2009 IEEE 9th Malaysia International Conference on Communications (MICC), 2009, pp. 703–708.